Hindawi
Journal of Chemistry
Volume 2017, Article ID 3831507, 8 pages
https://doi.org/10.1155/2017/3831507

Research Article

Investigation of Antimicrobial, Antioxidant, and DNA Binding Studies of Bioactive Cu(II), Zn(II), Co(II), and Ni(II) Complexes of Pyrimidine Derivative Schiff Base Ligand

Shahul Hameed Sukkur Saleem,[1,2] Murugesan Sankarganesh,[1] Paul Raj Adwin Jose,[1,2] Karunganathan Sakthikumar,[1] Liviu Mitu,[3] and Jeyaraj Dhaveethu Raja[1]

[1]*Chemistry Research Centre, Mohamed Sathak Engineering College, Kilakarai, Tamilnadu 623806, India*
[2]*Research and Development Centre, Bharathiar University, Coimbatore, Tamilnadu 641046, India*
[3]*Department of Nature Sciences, University of Pitesti, 110040 Pitesti, Romania*

Correspondence should be addressed to Liviu Mitu; ktm7ro@yahoo.com and Jeyaraj Dhaveethu Raja; jdrajapriya@gmail.com

Received 23 July 2017; Revised 5 September 2017; Accepted 1 October 2017; Published 20 November 2017

Academic Editor: Henryk Kozlowski

A new pyrimidine based Schiff base ligand (**HL**) and its four complexes of type $[MLOAc]\cdot n H_2O$ (Cu(II), **1**; Zn(II), **2**; Co(II), **3**; and Ni(II), **4**) have been synthesized and characterized by elemental analysis, MS, ^{1}H-NMR, FT-IR, UV-visible, and ESR techniques. The electronic and ESR spectral data suggested that complexes **1**–**4** possess square planar geometry. Antimicrobial activities of **HL** and complexes **1**–**4** were tested against four bacteria *(Staphylococcus aureus*, *Staphylococcus pneumonia*, *Salmonella enterica typhi*, and *Haemophilus influenzae)* and two fungal strains *(Aspergillus flavus* and *Aspergillus niger)*. These results show that complexes **1**–**4** have good antimicrobial activity compared to **HL**. The DNA cleavage activity of **HL** and complexes **1**–**4** was monitored by the agarose gel electrophoresis method. The antioxidant property of the prepared compounds was assessed by using 2,2′-diphenyl-1-picrylhydrazyl (DPPH) free radical scavenging method. DNA binding properties of **HL** and complexes **1**–**4** have been investigated by electronic absorption technique and viscometric measurements.

1. Introduction

Schiff base ligand is considered as a trendiest base because of its various applications like catalytic, optical, electronic, antibacterial, antifungal, antiviral, anti-inflammatory, and antitumor activities [1–5]. Transition metals play a more important role in drug design because of their biologically active metal ions and ligands [6]. When they are chelated with Schiff base ligand, the biological activity of the metal ions was significantly increased based on the geometry, reactivity, and functional group present in the ligand. Coordination of such ligands with metal ions likewise, copper, zinc, cobalt, and nickel, has antimicrobial, antioxidant, and DNA interaction properties [7, 8]. Moreover, Schiff base ligand is synthesized from pyrimidine derivatives that are much more of interest, because the pyrimidine is a heterocyclic compound, which also is present in nucleic acids [9]. These pyrimidine derivatives drugs are used in antimicrobial and anticancer related diseases [10, 11]. Similarly, salicylaldehyde derived Schiff base ligand exhibits better biological properties and its transition metal complexes increased biological activities [12].

In this research framework, we have synthesized the Cu(II), Zn(II), Co(II), and Ni(II) complexes with Schiff base ligand from pyrimidine and salicylaldehyde derivatives. They are characterized by different spectral and analytical methods and also their antimicrobial, antioxidant, and DNA binding properties were studied.

2. Experimental

2.1. Materials and Methods. 2,5-Dihydroxybenzaldehyde, 2-amino-4,6-dimethoxypyrimidine, $Cu(CH_3COO)_2\cdot H_2O$,

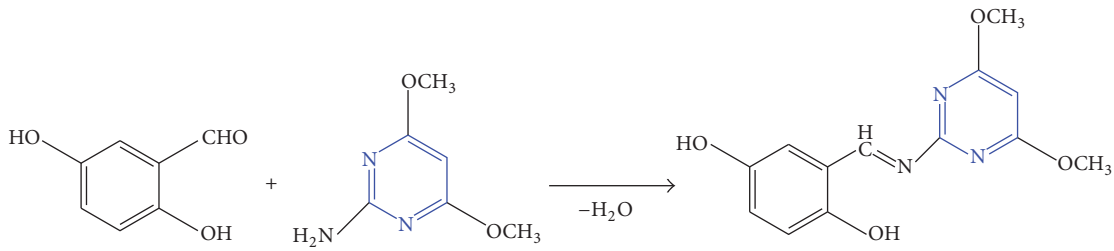

Scheme 1: Synthetic route of ligand **HL**.

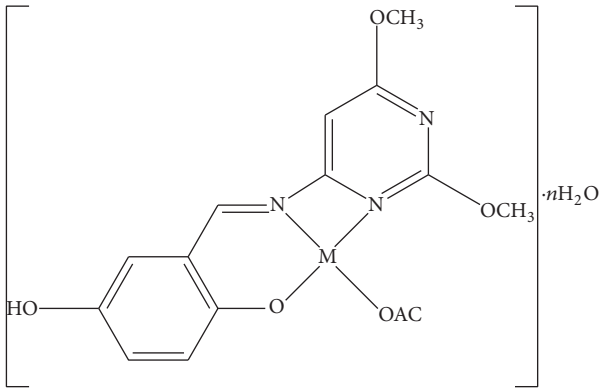

M = Cu(II) **1**, Zn(II) **2**, Co(II) **3** and Ni(II) **4**
n = 1 or 2

Scheme 2: Proposed structure of complexes **1–4**.

$Zn(CH_3COO)_2{\cdot}2H_2O$, $Co(CH_3COO)_2{\cdot}2H_2O$, $Ni(CH_3COO)_2{\cdot}2H_2O$, deoxyribose nucleic acid from calf thymus CT DNA, agarose gel, Tris-HCl, Tris-buffer, sodium chloride, bromophenol blue, and ethidium bromide were procured form Sigma Aldrich and Alfa Aesar company.

2.2. Instruments. The electronic spectra and absorption spectral titration were recorded on a UV-Visible-1800 (Shimadzu) spectrophotometer and the IR spectra were done in KBr pellets on a FTIR (Shimadzu, IR Affinity-1) spectrometer. The mass and ^{1}H-NMR spectra were recorded on an ESI-MS spectrometer, IIT Bombay, and Bruker Avance DRX 300 FT-NMR spectrometer, IISC, Bangalore. The DNA cleavage studies were carried out in DMSO solution using UV-transilluminator.

2.3. Synthesis of Ligand HL. An ethanolic solution (10 mL) of 2,5-dihydroxybenzaldehyde (2 mmol) was added to the ethanolic solution (15 mL) of 2-amino-4,6-dimethoxypyrimidine (2 mmol) and next the mixture was refluxed for one hour. After solution was evaporated slowly on a water bath and finally reddish-brown solid was obtained and washed with ethanol and dried in vacuo (Scheme 1).

*2.4. Synthesis of Complexes **1–4**.* A solution of **HL** (1 mmol) in methanol (40 mL) was added slowly to a solution of metal(II) acetate salts (1 mmol) in methanol (30 mL) with constant stirring. The reaction mixture was refluxed for 2 hours. Then, the resultant solution was evaporated slowly on a water bath and finally a solid product was obtained and washed with cold ethanol and dried in vacuo (Scheme 2).

2.5. Antimicrobial Assay. Antimicrobial activities of the **HL** and complexes **1–4** were screened against the four different bacteria, *Staphylococcus aureus (S. aureus)*, *Staphylococcus pneumonia (S. pneumonia)*, *Salmonella enterica typhi (S. typhi)*, *and Haemophilus influenzae (H. influenzae)*, and two fungi, *Aspergillus flavus (A. flavus)* and *Aspergillus niger (A. niger)* strains by the well diffusion method [13]. Sparfloxacin (antibacterial) and Ketoconazole (antifungal) were used as standard drugs.

2.6. Antioxidant Study. Antioxidant activity of **HL** and complexes **1–4** were studied by DPPH scavenging method [14]. The % inhibition was calculated according to the following formula:

$$\%\ \text{Inhibition} = \left[\frac{A_0 - A_1}{A_1}\right] \times 100, \tag{1}$$

where A_0 is the absorbance control and A_1 is the absorbance of sample or standard.

2.7. DNA Cleavage Study. DNA cleavage activities of **HL** and complexes **1–4** with CT-DNA were demonstrated by agarose gel electrophoresis method as reported earlier [15].

2.8. DNA Interaction Studies. DNA interaction studies of **HL** and complexes **1–4** with CT-DNA in Tris-HCl buffer were analyzed by electronic absorption spectral titration and viscometric measurements [16, 17].

3. Results and Discussions

The newly synthesized **HL** and complexes **1–4** were found to be intensely coloured. The analytical data and physical properties of the prepared compounds are listed in Table 1. The low molar conductivity of the complexes **1–4** (9.72, **1**; 10.80, **2**; 11.60, **3**; and 12.4, **4** $\text{ohm}^{-1}\,\text{cm}^2\,\text{mol}^{-1}$) shows that they is nonelectrolytic nature due to lack of dissociation.

3.1. Mass Spectra. Mass spectra of the **HL** and complexes **1–4** recorded at room temperature were used to compare their stoichiometry composition. The ligand **HL** showed a molecular ion peak at (m/z 276) corresponding to $C_{13}H_{13}N_3O_4$. The molecular ion peaks for the complexes **1–4** observed at m/z

Table 1: Analytical and physical data of the ligand **HL** and complexes **1**–**4**.

Compounds	Molecular formula	Colour	Yield %	M.P. °C	Calc. (Found) %			
					C	H	N	M
HL	$C_{13}H_{13}N_3O_4$	brown	84	260	56.87 (56.09)	4.71 (4.65)	15.21 (15.01)	—
1	$CuC_{15}H_{15}N_3O_6$	brown	78	282	45.40 (45.38)	3.81 (3.62)	10.59 (10.54)	16.01 (16.00)
2	$ZnC_{15}H_{15}N_3O_6$	brown	79	278	45.19 (45.08)	3.79 (3.71)	10.54 (10.49)	16.40 (16.38)
3	$CoC_{15}H_{15}N_3O_6$	red	82	295	45.93 (45.89)	3.85 (3.79)	10.71 (10.68)	15.73 (15.69)
4	$NiC_{15}H_{15}N_3O_6$	brown	74	271	45.96 (45.89)	3.86 (3.81)	10.72 (10.68)	14.97 (14.89)

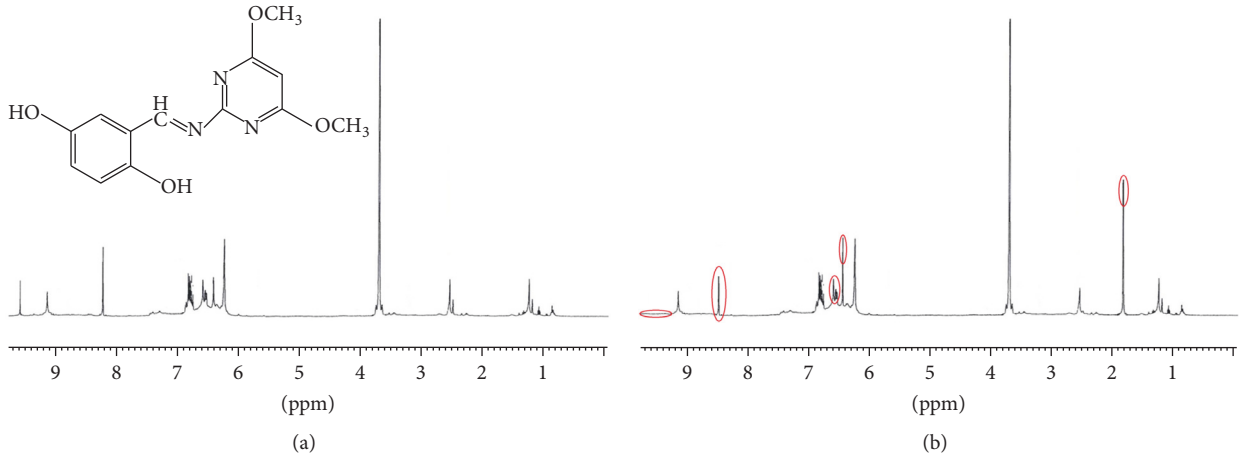

Figure 1: ^{1}H-NMR spectra of (a) ligand **HL** and (b) complex **2**.

396, **1**; 398, **2**; 392, **3**; and 391, **4** confirms the stoichiometry of metal chelates as [ML] type and 1 : 1 ratio.

3.2. ^{1}H-NMR Spectra. The ^{1}H-NMR spectra of the **HL** and complex **2** show the signals and are summarized in Table 2 and Figure 1. In free ligand **HL**, the azomethine proton at 8.2 (s) ppm, pyrimidine proton at 6.45 (s) ppm, aromatic -CH protons at 6.8–6.23 (m) ppm, -OCH_3 protons at 3.73 (s), and phenolic -OH protons (C_2 and C_5) appeared at 9.58 (s) and 9.12 (s). After the complexation, the azomethine proton signal was shifted toward the downfield region at 8.5 (s) and -OH proton (C_2) is disappeared. These results suggest that the phenolic oxygen (C_2), azomethine, and pyrimidine nitrogen atoms are taking part in the complexation and there is no appreciable change in all other signals in this complex. In complex **2**, a new peak is observed at 1.83 (s) due to acetate molecule involved in the complexation.

3.3. IR Spectra. IR spectral data of **HL** and complexes **1**–**4** are shown in Table 3. IR spectrum of **HL** showed that a strong sharp band observed at 1564 cm^{-1} [18] is assigned to the azomethine group (-HC=N-), which was shifted to lower frequencies in the spectra of complexes **1**–**4** indicating that the involvement of azomethine nitrogen in coordination with the central metal ion and pyrimidine (C=N) band appeared at 1465 cm^{-1} which was shifted towards lower frequencies and in the range of 1465–1442 cm^{-1} due to the fact that pyrimidine nitrogen atom is one of the coordination sites around the central metal ion. In all metal complexes, carboxylate of the acetate group (CH_3COO^-) is strongly absorbed (symmetry) in the range of 1640–1668 cm^{-1} and (asymmetry) more weakly at 1402–1428 cm^{-1}. The bands appeared in the region of 450–434 cm^{-1} were assigned to $\nu_{(M\text{-}N)}$ for complexes **1**–**4**, indicating that the imine and pyrimidine nitrogen atoms are involved coordination with central metal ions [19]. The bands observed in the region of 497–502 cm^{-1} were assigned to $\nu_{(M\text{-}O)}$ for complexes **1**–**4**, indicating that the phenolic oxygen atom was involved in coordination with central metal ions [20].

3.4. Electronic Spectra. Electronic absorption data of **HL** and complexes **1**–**4** are depicted in Table 4. In the absorption spectra of **HL**, intense absorption bands at 292 and 370 nm were attributed to π-π^* and n-π^* transitions (Table 1) [21]. For complex **1**, the bands appeared at 482 and 620 nm, which were assigned to the $^2B_{1g} \rightarrow {}^2E_g$ transition and this indicates the square planar geometry [22]. Complex **2** has d^{10} configuration, which suggests the absence of d-d transition

Table 2: ^{1}H-NMR spectral data of the ligand **HL** and complex **2**.

Compounds	-O-CH_3 (δ)	Aromatic -CH (δ)	Pyrimidine -CH (δ)	Phenolic -OH (δ)	CH=N (δ)	CH_3COO^- (δ)
HL	3.73 (s)	6.8–6.23 (m)	6.45	9.12 (C_5) 9.58 (C_2)	8.2	—
Complex **2**	3.73 (s)	6.8–6.23 (m)	6.5	9.14	8.5	1.83

Table 3: Infrared spectral data of the ligand **HL** and complexes **1**–**4** (cm^{-1}).

Compounds	CH=N	Pyrimidine C=N	-OAc	-OH	M-N	M-O
HL	1564	1465	—	3368	—	—
1	1540	1442	1668	3364	434	497
2	1542	1445	1648	3360	447	498
3	1544	1448	1652	3363	460	504
4	1548	1446	1665	3371	450	502

Table 4: Electronic spectral data of the synthesized compounds.

Compounds	λ_{max}, cm^{-1}	Band assignment	Suggested geometry
HL	292 370	INCT*	—
1	482 620	$^2B_{1g} \rightarrow {}^2E_g$	Square planar
2	310 380	INCT*	Square planar
3	428 465	$^1A_{1g} \rightarrow {}^1B_{1g}$	Square planar
4	432 446	$^1A_{1g} \rightarrow {}^1A_{2g}$	Square planar

*Intraligand charge transfer.

bands, so complex **2** reveals that INCT bands shift at 310 and 380 nm, respectively; this indicates the formation of zinc complex [14]. For complex **3**, the bands appeared at 428 and 465 nm which were attributable to the $^1A_{1g} \rightarrow {}^1B_{1g}$ transition in a square planar geometry [23]. For complex **4**, the bands are examined at 432 and 446 cm^{-1}, which were attributed to $^1A_{1g} \rightarrow {}^1A_{2g}$ transition and this shows square planar geometry around the central metal atom [24].

3.5. ESR Spectra. The X-band ESR spectra of complex **1** were recorded in DMSO at room and liquid nitrogen temperature (Figure 2). The frozen solution spectrum shows well resolved four-line spectral lines. The results are summarized in Table 5. The spin Hamiltonian parameters have been calculated by Kivelson's method. The observed g-values are in the order $g_\parallel(2.11) > g_\perp(2.04) > g_e(2.0027)$ indicating that the unpaired electron lies predominantly in $d_{x2\text{-}y2}$ orbital of Cu(II) ion [25]. These results also supported the square planar geometry around the central metal(II) ion. The interaction coupling constant G value is calculated from the following:

$$G = \frac{g_\parallel - 2.00277}{g_\perp - 2.00277}. \quad (2)$$

The observed G value of 4.184 shows that no interaction between Cu-Cu is centred in the solid state of the Cu(II) complex [26]. If the G value is greater than 4, the exchange interaction is negligible.

3.6. Antimicrobial. Antibacterial activities of **HL** and complexes **1**–**4** were screened against the four different bacteria, *Staphylococcus aureus (S. aureus)*, *Staphylococcus pneumonia (S. pneumonia)*, *Salmonella typhi (S. typhi)*, and *Haemophilus influenzae (H. influenzae)*, and Sparfloxacin (standard drug). The zone of inhibition and minimum inhibitory concentration (MIC) values of synthesized compounds against bacteria are given in Figures 3(a) and 4(a). From the above data, complexes **1** and **3** have good antibacterial activity compared to **HL** and complexes **2** and **4**. Moreover, zone of inhibitory efficiency of synthesized compounds is higher in *S. aureus* bacteria as compared to other bacterial strains.

Antifungal activities of **HL** and complexes **1**–**4** were screened against two different fungi, *Aspergillus flavus (A. flavus)* and *Aspergillus niger (A. niger)* strains. Ketoconazole was used as standard drug. The zone of inhibition and minimum inhibitory concentration (MIC) values of synthesized compounds against fungal strains are given in Figures 3(b) and 4(b). From the above data, complexes **1** and **3** have

Table 5: The ESR spectral data for complex **1**.

Compound	g tensor			Hyperfine constant $\times 10^4$ cm^{-1}			G
	$g_\parallel$	$g_\perp$	g_{av}	$A_\parallel$	$A_\perp$	A_{iso}	
1	2.11	2.04	2.06	80	25	43.3	4.184

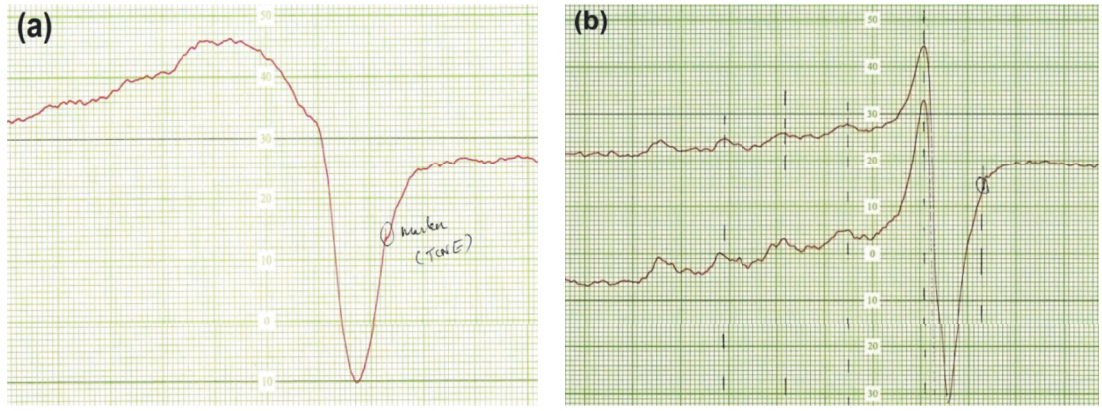

(a) (b)

Figure 2: ESR spectra of complex **1**: (a) RT and (b) LNT.

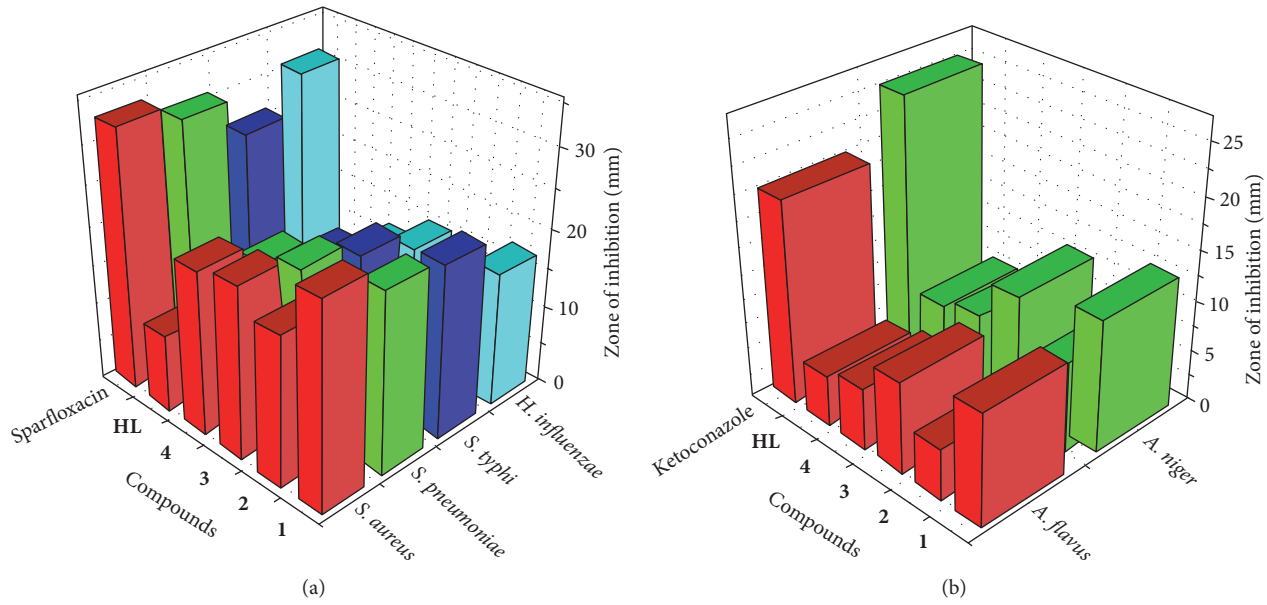

Figure 3: Antimicrobial activity of ligand **HL** and complexes **1**–**4**: (a) antibacterial; (b) antifungal.

good antifungal activity compared to **HL** and complexes **2** and **4**. Moreover, zone of inhibitory effect of newly prepared compounds is higher in *A. niger* fungi as compared to *A. flavus*.

3.7. Antioxidant. The antioxidant activities of **HL** and complexes **1**–**4** were analyzed by using DPPH stable free radical and are depicted in Figure 5. This experiment was carried out by using UV-visible spectroscopy; results suggest that the absorption peak intensity decreases and disappears because of the addition of newly prepared compounds. Hence, the synthesized compounds can donate the hydrogen atom to DPPH free radical and color of the compounds changes from purple to yellow. The results have suggested that complexes **1** and **3** have good scavenging ability **HL** and complexes **2** and **4**.

3.8. DNA Cleavage. DNA cleavage studies of **HL** and complexes **1**–**4** with CT-DNA in the presence of hydrogen peroxide (H_2O_2) were analyzed by agarose gel electrophoresis techniques (Figure 6). From Figure 6, complex **1** has good DNA damage activity compared to ligand **HL** and complexes

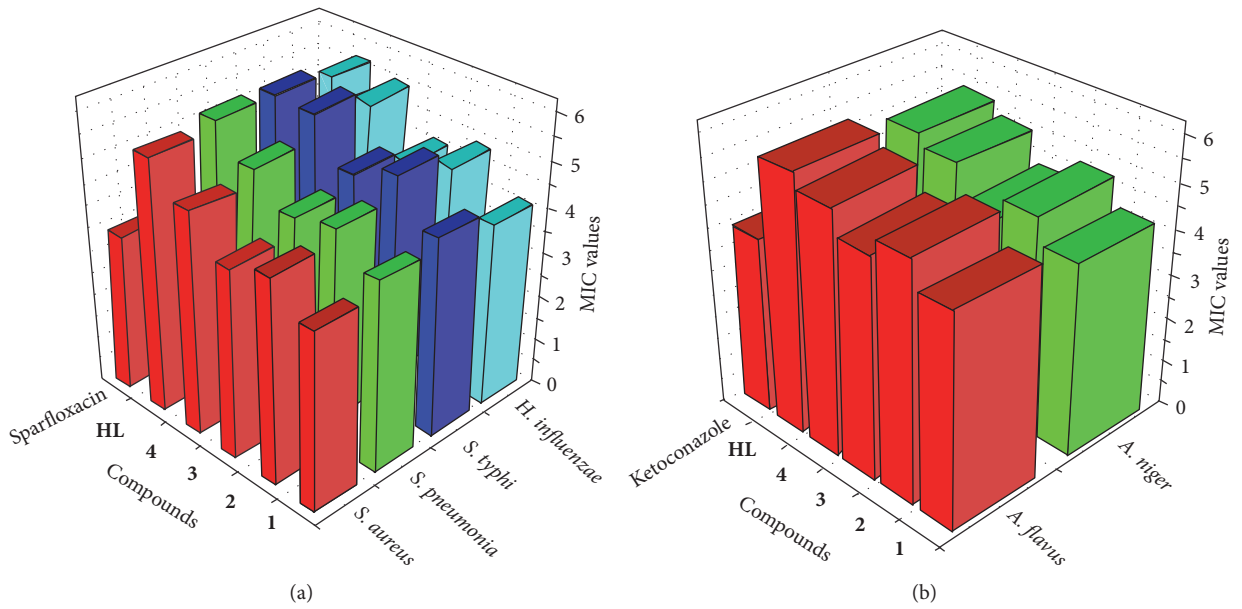

Figure 4: Minimum inhibitory concentration of ligand **HL** and complexes **1**–**4** (10^{-2} M): (a) antibacterial; (b) antifungal.

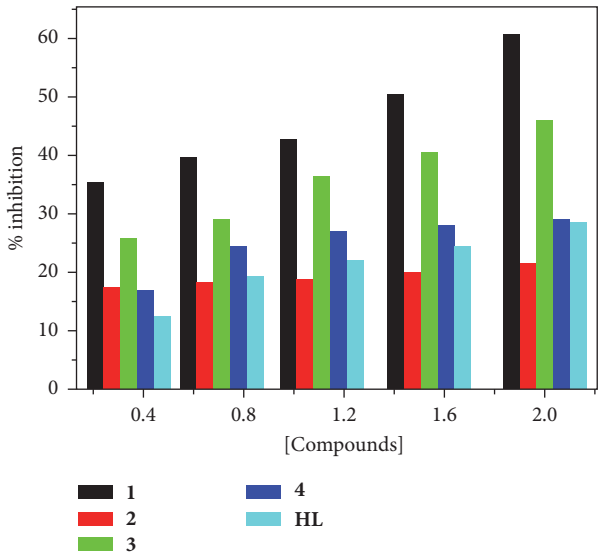

Figure 5: % inhibition of **HL** and complexes **1**–**4** with DPPPH free radical.

Figure 6: Agarose gel diagram showing cleavage of CT-DNA by ligand **HL** and complexes **1**–**4** at RT. Lane 1: DNA control + H_2O_2; Lane 2: DNA + **HL** + H_2O_2; Lane 3: DNA + **1** + H_2O_2; Lane 4: DNA + **2** + H_2O_2; Lane 5: DNA + **3** + H_2O_2; Lane 6: DNA + **4** + H_2O_2.

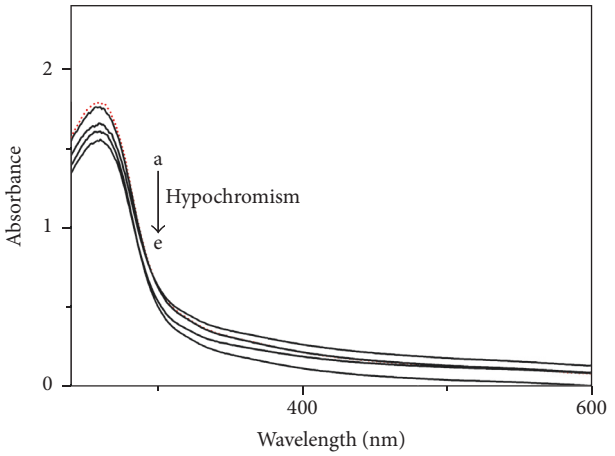

Figure 7: Absorption spectra of complex **1** with CT-DNA in Tris-HCl buffer.

2–**4**. These results reveal that complex **1** is involved in the formation of hydroxyl radicals which may damage DNA via Fenton-type mechanism.

3.9. DNA Interaction

3.9.1. Absorption Spectral Titration. Absorption spectroscopy is one of the most common methods for determining the binding mode of CT-DNA with complexes. The absorption spectra of complex **1** in the presence and absence of CT-DNA with different concentration in Tris-HCl buffer are depicted in Figure 7. The increasing concentration of CT-DNA to the fixed concentration of complexes **1**–**4**, the hypochromism, and slight red shift have been observed. Clearly, these obtained results are coinciding with the previously reported results [27] which suggest that the **HL** and complexes

Table 6: Absorption spectral properties of **HL** and complexes **1–4** with CT-DNA.

Compounds	Free λ_{max} (nm)	Bound λ_{max} (nm)	Red shift $\Delta\lambda$	Type of chromism	Hypochromism (%)	Binding constant (K_b)
HL	293	294	01	Hypochromism and red shift	22.45	1.06×10^4
1	298	304	06	Hypochromism and red shift	40.82	4.76×10^5
2	300	305	05	Hypochromism and red shift	29.38	9.28×10^4
3	302	307	05	Hypochromism and red shift	38.74	1.27×10^5
4	301	306	05	Hypochromism and red shift	35.42	1.02×10^5

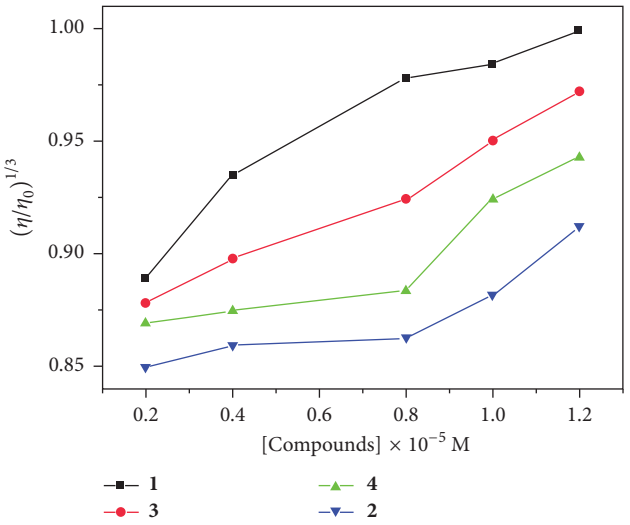

Figure 8: Effect of increasing concentration of complexes **1–4** on the relative viscosity of CT-DNA.

1–4 interact with CT-DNA via intercalation mode. The intrinsic binding constant (K_b) of **HL** and complexes **1–4** was determined by using the following formula (Table 6): $[DNA]/\varepsilon_a - \varepsilon_f = [DNA]/\varepsilon_b - \varepsilon_f + [K_b(\varepsilon_b - \varepsilon_f)]^{-1}$, where [DNA] is the concentration of base pairs of DNA. The apparent absorption coefficients ε_a, ε_f, and ε_b correspond to $A_{obs.}/[M]$, the extinction coefficient for the free complex, and extinction coefficient for the complex in the fully bound form, respectively. The K_b values of **HL** and complexes **1–4** are in the following order: **1** (4.76×10^5) > **3** (1.27×10^5) > **4** (1.02×10^5) > **2** (9.28×10^4) > **HL** (1.06×10^4).

3.9.2. Viscometric Measurements. To clarify the binding mode of newly synthesized compounds with CT-DNA by using viscometric measurements, the plots of relative viscosity versus [complex]/[DNA] (Figure 8) show that the viscous flow of DNA increases when increasing the concentration of **HL** and complexes **1–4**. These results have suggested the interaction of compounds with DNA via intercalation binding mode.

4. Conclusions

In summary, we have successfully synthesized the Cu(II), Zn(II), Co(II), and Ni(II) complexes of Schiff base ligand bearing pyrimidine derivatives. The newly synthesized compounds were analyzed by various spectral and analytical techniques. The elemental and mass spectral results support that the stoichiometry of complexes **1–4** is of 1:1 ratio and the type is ML. All the spectral results suggest that complexes **1–4** possess square planar geometry around the central metal atom. Antimicrobial and antioxidant results reveal that complexes **1** and **3** have good antimicrobial and the ability to scavenge DPPH radicals compared to ligand **HL** and complexes **2** and **4**. Complex **1** has good DNA cleavage ability compared to **HL** and complexes **2–4**. DNA interactions studies results have suggested that the newly prepared compounds interact with CT-DNA via intercalation mode.

Conflicts of Interest

The authors declare that they have no conflicts of interest regarding the publication of this paper.

Acknowledgments

The authors express their heartfelt gratitude to the Department of Science and Technology (DST), Science and Engineering Research Board (SERB-Ref. no. SR/FT/CS-117/2011, dated 29.06.2012), New Delhi, for financial assistance and also express deepest gratitude to the Managing Board, Principal, and Chemistry Research Centre, Mohamed Sathak Engineering College, Kilakarai, for providing research facilities and constant encouragements.

References

[1] B. Zhang, S. Li, E. Herdtweck, and F. E. Kühn, "Schiff base complexes of methyltrioxorhenium (VII): Synthesis and catalytic application," *Journal of Organometallic Chemistry*, vol. 739, pp. 63–68, 2013.

[2] M. K. Taylor, J. Reglinski, and D. Wallace, "Coordination geometry of tetradentate Schiff's base nickel complexes: The effects of donors, backbone length and hydrogenation," *Polyhedron*, vol. 23, no. 18, pp. 3201–3209, 2004.

[3] H.-C. Wu, P. Thanasekaran, C.-H. Tsai et al., "Self-assembly, reorganization, and photophysical properties of silver(I)-Schiff-base molecular rectangle and polymeric array species," *Inorganic Chemistry*, vol. 45, no. 1, pp. 295–303, 2006.

[4] E. Kwiatkowski, G. Romanowski, W. Nowicki, M. Kwiatkowski, and K. Suwińska, "Chiral dioxovanadium(V) complexes with single condensation products of 1,2-diaminocyclohexane and

aromatic o-hydroxycarbonyl compounds: Synthesis, characterization, catalytic properties and structure," *Polyhedron*, vol. 26, no. 12, pp. 2559–2568, 2007.

[5] N. K. Chaudhary and P. Mishra, "Metal complexes of a novel schiff base based on penicillin: characterization, molecular modeling, and antibacterial activity study," *Bioinorganic Chemistry and Applications*, vol. 2017, Article ID 6927675, 13 pages, 2017.

[6] N. A. Negm, M. F. Zaki, and M. A. I. Salem, "Cationic schiff base amphiphiles and their metal complexes: Surface and biocidal activities against bacteria and fungi," *Colloids and Surfaces B: Biointerfaces*, vol. 77, no. 1, pp. 96–103, 2010.

[7] T. Arun, R. Subramanian, and N. Raman, "Novel bio-essential metal based complexes linked by heterocyclic ligand: Synthesis, structural elucidation, biological investigation and docking analysis," *Journal of Photochemistry and Photobiology B: Biology*, vol. 154, pp. 67–76, 2016.

[8] A. Y. Lukmantara, D. S. Kalinowski, N. Kumar, and D. R. Richardson, "Synthesis and biological evaluation of 2-benzoylpyridine thiosemicarbazones in a dimeric system: Structure-activity relationship studies on their anti-proliferative and iron chelation efficacy," *Journal of Inorganic Biochemistry*, vol. 141, no. 1, pp. 43–54, 2014.

[9] J. Hung and L. M. Werbel, "Investigations into the synthesis of 6-ethyl-5-(4-pyridinyl)-2,4-pyrimidinediamine as a potential antimalarial agent," *Journal of Heterocyclic Chemistry*, vol. 21, no. 3, pp. 741–744, 1984.

[10] R. S. Herbst, J. V. Heymach, M. S. Oreilly, A. Onn, and A. Ryan, "Investigations into the synthesis of 6-ethyl-5-(4-pyridinyl)-2, 4-pyrimidinediamine as a potential antimalarial agent," *Expert Opinion on Investigational Drugs*, vol. 16, pp. 239–249, 2007.

[11] H. Bayrak, A. Demirbas, S. A. Karaoglu, and N. Demirbas, "Synthesis of some new 1,2,4-triazoles, their Mannich and Schiff bases and evaluation of their antimicrobial activities," *European Journal of Medicinal Chemistry*, vol. 44, no. 3, pp. 1057–1066, 2009.

[12] B.-L. Fei, W.-S. Xu, H.-W. Tao et al., "Effects of copper ions on DNA binding and cytotoxic activity of a chiral salicylidene Schiff base," *Journal of Photochemistry and Photobiology B: Biology*, vol. 132, pp. 36–44, 2014.

[13] N. Raman, J. D. Raja, and A. Sakthivel, "Synthesis, spectral characterization of Schiff base transition metal complexes: DNA cleavage and antimicrobial activity studies," *Journal of Chemical Sciences*, vol. 119, no. 4, pp. 303–310, 2007.

[14] N. Revathi, M. Sankarganesh, J. Rajesh, and J. D. Raja, "Biologically Active Cu(II), Co(II), Ni(II) and Zn(II) Complexes of Pyrimidine Derivative Schiff Base: DNA Binding, Antioxidant, Antibacterial and In Vitro Anticancer Studies," *Journal of Fluorescence*, vol. 27, no. 5, pp. 1801–1814, 2017.

[15] N. Raman, S. J. Raja, J. Joseph, and J. D. Raja, "Molecular designing, structural elucidation, and comparison of the cleavage ability of oxovanadium(IV) Schiff base complexes," *Russian Journal of Coordination Chemistry*, vol. 33, no. 1, pp. 7–11, 2007.

[16] A. Gubendran, M. P. Kesavan, S. Ayyanaar, J. D. Raja, P. Athappan, and J. Rajesh, "Synthesis and characterization of water-soluble copper(II), cobalt(II) and zinc(II) complexes derived from 8-hydroxyquinoline-5-sulfonic acid: DNA binding and cleavage studies," *Applied Organometallic Chemistry*, article e3708, 2017.

[17] M. P. Kesavan, G. G. Vinoth Kumar, J. Dhaveethu Raja, K. Anitha, S. Karthikeyan, and J. Rajesh, "DNA interaction, antimicrobial, antioxidant and anticancer studies on Cu(II) complexes of Luotonin A," *Journal of Photochemistry and Photobiology B: Biology*, vol. 167, pp. 20–28, 2017.

[18] R. M. Silverstein, G. C. Bassler, and T. C. Morrill, *Spectrometric Identification of Organic Compounds*, New York, NY, USA, 4th edition, 1981.

[19] M. Thomas, M. K. M. Nair, and P. K. Radhakrishnan, "Rare Earth Iodide Complexes of 4–(2', 4 '-Dihydroxyphenylazo)Antipyrine," *Synthesis and Reactivity in Inorganic, Metal-Organic, and Nano-Metal Chemistry*, vol. 25, no. 3, pp. 471–479, 1995.

[20] N. Raman, J. Dhaveethu Raja, and A. Sakthivel, "Template synthesis of novel 14-membered tetraazamacrocyclic transition metal complexes: DNA cleavage and antimicrobial studies," *Journal of the Chilean Chemical Society*, vol. 53, no. 3, pp. 1568–1571, 2008.

[21] R. F. M. Elshaarawy, Z. H. Kheiralla, A. A. Rushdy, and C. Janiak, "New water soluble bis-imidazolium salts with a saldach scaffold: Synthesis, characterization and in vitro cytotoxicity/bactericidal studies," *Inorganica Chimica Acta*, vol. 421, pp. 110–122, 2014.

[22] J. A. Faniran, K. S. Patel, and L. O. Nelson, "Physico-chemical studies of metal β-diketonates-I Infrared spectra of 1-(3-pyridyl)-1,3-butanedione and its divalent metal complexes," *Journal of Inorganic and Nuclear Chemistry*, vol. 38, no. 1, pp. 77–80, 1976.

[23] N. Raman, J. Dhaveethu Raja, and A. Sakthivel, "Template synthesis of novel 14-membered tetraazamacrocyclic transition metal complexes: DNA cleavage and antimicrobial studies," *Journal of the Chilean Chemical Society*, vol. 53, no. 3, pp. 1–4, 2008.

[24] A. Kumar, A. K. Jha, N. Mazumdar et al., "Complexes of nickel(II), zinc(II), palladium(II) and cadmium(II) with some furan-2-thiohydrazones," *Journal of the Indian Chemical Society*, vol. 74, article 485, 1997.

[25] N. Raman, A. Sakthivel, J. D. Raja, and K. Rajasekaran, "Designing, structural elucidation and comparison of the cleavage ability of metal complexes containing tetradentate Schiff bases," *Russian Journal of Inorganic Chemistry*, vol. 53, no. 2, pp. 213–219, 2008.

[26] H. Montgomery and E. C. Lingafelter, "The crystal structure of Tutton's salts. IV. Cadmium ammonium sulfate hexahydrate," *Acta Crystallographica*, vol. 20, no. 6, pp. 728–730, 1966.

[27] N. Shahabadi, S. Kashanian, and F. Darabi, "In Vitro study of DNA interaction with a water-soluble dinitrogen schiff base," *DNA and Cell Biology*, vol. 28, no. 11, pp. 589–596, 2009.